Novel Phosphovanadate Layered Structure Assembled from a Tetrametallic Cubane-Like V^V Cluster

Fa-Nian Shi,[a] Filipe A. Almeida Paz,[b] João Rocha,*[a] Jacek Klinowski,[b] and Tito Trindade[a]

Keywords: Organic-inorganic hybrid / Hydrothermal synthesis / Oxo ligands / Vanadium

A novel phosphovanadate layered structure intercalated by 4,4′-bipyridinium cations, $(C_{10}H_{10}N_2)[(VO_2)_4(PO_4)_2]$, was synthesised under hydrothermal conditions and its crystal structure determined using single-crystal X-ray diffraction. The anionic $[(VO_2)_4(PO_4)_2]_n^{2n-}$ perforated layers are strongly hydrogen bonded to the interlayer 4,4′-bipyridinium cations and are assembled by an unprecedented secondary tetrametallic V^V building unit constructed from a distorted cubane-like $\{V_4O_4\}$ cluster. The compound was further characterised by IR, Raman, ^1H, ^1H-^{13}C, ^{31}P and ^{51}V MAS NMR spectroscopy, and by thermal and elemental analysis.

Introduction

Much attention has been given to the synthesis of organic-inorganic hybrid compounds given their ability to combine features from both organic and inorganic building units, leading to novel materials with interesting architectures and potential applications. Vanadium, one of the most versatile transition metals through the combination of its three distinct oxidation states with the several possible coordination geometries,[1] has been extensively used as one of the primary building blocks in transition metal phosphates, which can be employed in functional materials due to their unusual catalytic, magnetic, electrical and optical properties.[2] Solvothermal synthetic conditions provide a versatile route for the synthesis of such materials; organic molecules are usually added to the reactive mixtures. These molecules can coordinate to the metal centres,[3] or act as structure-directing agents, templates, counterions or simply as space-filling molecules.[1,4] In this context, special interest has been given to layered structures and their intercalation by a variety of guest molecules.[1]

Following our interest in hybrid materials containing bridging organic ligands[5,6] and, in particular, vanadium centres,[6,7] we wish to report the preparation and structural characterisation of a novel phosphovanadate layered structure intercalated by 4,4′-bipyridinium cations, $(C_{10}H_{10}N_2)[(VO_2)_4(PO_4)_2]$ (**I**). The anionic layers are assembled by an unprecedented secondary tetrametallic V^V building unit that exhibits a distorted cubane-type structural motif. Other tetrametallic vanadium cores of the $\{V_4O_4\}$ type have already been investigated: those that exhibit the boat conformation (involving two pairs of edge-sharing octahedra connected by two corner-sharing oxygen atoms) or the chair conformation (where each VO_6 octahedron is edge-shared by two neighbouring octahedra).[8] Although the formation of cubane-type clusters is a characteristic structural motif in the coordination chemistry of many different metal centres,[9] only vanadium thiocubane clusters $\{V_4S_4\}$ have been described.[10] Thus, to the best of our knowledge, compound **I** is the first material containing such a structural motif assembled by VO_6 octahedra that are further bridged by phosphate groups (Scheme 1).

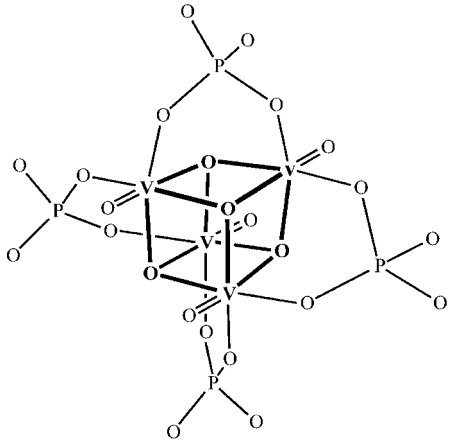

Scheme 1

[a] Department of Chemistry, University of Aveiro, CICECO, 3810-193 Aveiro, Portugal
E-mail: rocha@dq.ua.pt
[b] Department of Chemistry, University of Cambridge, Lensfield Road, Cambridge CB2 1EW, U.K.
E-mail: jk18@cam.ac.uk

Results and Discussion

Crystal Description

The product of the hydrothermal reaction between vanadium(v) oxide, phosphoric acid and 4,4′-bipyridine (4,4′-bpy; see Exp. Sect.) was analysed by single-crystal X-ray diffraction (Table 1) and elemental analysis, and formulated as $(C_{10}H_{10}N_2)[(VO_2)_4(PO_4)_2]$ (**I**) (where $C_{10}H_{10}N_2^{2+}$ = 4,4′-$bpyH_2^{2+}$ = 4,4′-bipyridinium). A direct comparison between the experimental powder X-ray diffraction (PXRD) pattern and a simulation based on single-crystal data confirms phase purity and homogeneity of the bulk sample, despite the presence of a few reflections attributed to strong preferential orientation of the compound.

Table 1. Crystal data and structure refinement information

Formula	$C_{10}H_{10}N_2O_{16}P_2V_4$
Molecular weight	679.90
Crystal system	Monoclinic
Space group	*P*2/c
a (Å)	14.797(3)
b (Å)	7.4178(15)
c (Å)	18.613(4)
β (°)	102.20(3)
Volume (Å^3)	1996.8(7)
Z	4
D_c (g cm^{-3})	2.262
μ(Mo-K_α) (mm^{-1})	2.063
F(000)	1336
Crystal size (mm)	0.12 × 0.12 × 0.10
Crystal type	orange blocks
θ range	3.54 to 27.48
Index ranges	$-19 \le h \le 18$
	$-8 \le k \le 9$
	$-19 \le l \le 24$
Reflections collected	11350
Independent reflections	4559 (R_{int} = 0.0583)
Final R_{int} [$I > 2\sigma(I)$]	$R1$ = 0.0463
	$wR2$ = 0.0888
Final R_{int} (all data)	$R1$ = 0.0805
	$wR2$ = 0.1022
Largest diff. peak and hole	0.641 and −0.666 e·Å^{-3}

The compound contains four crystallographically unique V^V centres distributed along two independent, but topologically identical, tetrametallic secondary building units (SBUs, {V(1),V(4)} and {V(2),V(3)}) that exhibit a distorted cubane-type structural motif (Figure 1) in which each VO_6 octahedron shares edges (belonging to the same face) with the three neighbouring octahedra (Figure 2). In these clusters, formed by twofold rotation axes perpendicu-

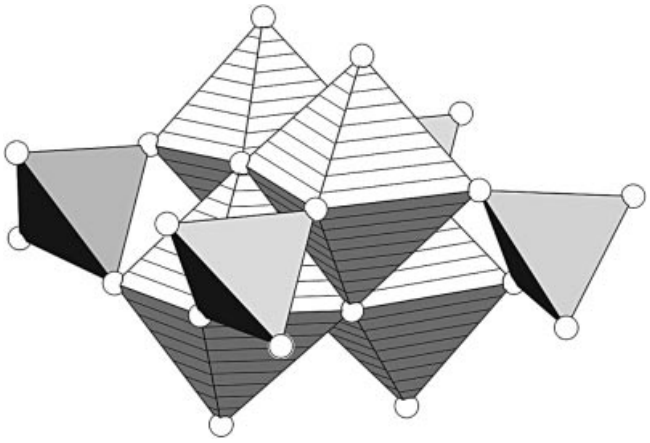

Figure 2. Polyhedral representation of a $\{(V_4O_8)(PO_4)_4\}$ secondary building unit; each VO_6 octahedron is edge-shared (from the same face) with the three neighbouring octahedra, leading to a tetrametallic tetrahedral V^V core

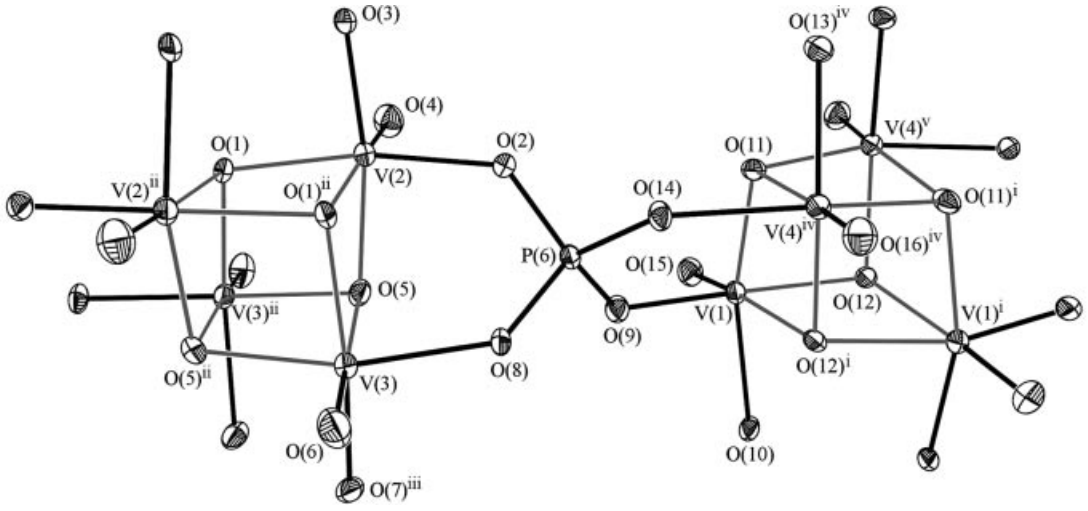

Figure 1. Tetrametallic secondary building units {V(1),V(4)} and {V(2),V(3)}, which form the two-dimensional perforated $[(VO_2)_4(PO_4)_2]_n^{2n-}$ anionic layer; atoms are represented as ellipsoids drawn at the 50% probability level; V···V distances within each SBU: V(1)···V(1)^i 3.3619(18) Å, V(1)···V(4)^{iv} 3.3593(12) Å, V(1)···V(4)^v 2.8031(11) Å, V(4)^{iv}···V(4)^v 3.3758(16) Å, V(2)···V(2)^{ii} 3.3543(16) Å, V(2)···V(3) 3.3322(11) Å, V(2)···V(3)^{ii} 2.8162(11) Å, V(3)···V(3)^{ii} 3.3628(18) Å; for bond lengths and angles see Tables 2 and 3; symmetry codes used to generate equivalent atoms: (i) 1 − *x*, *y*, 1/2 − *z*, (ii) −*x*, *y*, 1/2 − *z*, (iii) *x*, −1 + *y*, *z*, (iv) 1 − *x*, 1 + *y*, 1/2 − *z*, (v) *x*, 1 + *y*, *z*

lar to the *ac* plane, the coordination environment of each V^V centre resembles the typical 1+4+1 coordination type described by Boudin et al., with the observed short, intermediate and long (V−O) bonds within the expected ranges reported by the same authors (Table 2 and Table 3).[11] The core of each cluster consists of a tetrametallic V_4 tetrahedron: each face is capped by a μ_3−O ligand that is equatorially coordinated to two octahedra, $O_{equatorial}$, and also occupies the *trans* position to the oxo group of a third octahedron, O_{trans} (Figure 1). The registered V···V, V−$O_{equatorial}$ and V−O_{trans} distances are within the ranges, 2.8031(11)−3.3758(16) Å, 1.841(3)−1.933(3) Å and 2.426(3)−2.462(3) Å, respectively (Table 2; see caption of Figure 1 for detailed V···V distances). Phosphate groups appear with two distinct structural functions: on the one hand, within each SBU, they link adjacent V^V centres along the edges of the V_4 tetrahedra (Scheme 1, Figures 1 and 2); on the other hand, they establish physical links between adjacent V_4 tetrahedra. In fact, the parallel linking in the *ab* plane through the phosphate groups of the two previously mentioned SBUs leads to a two-dimensional (2D) anionic $[(VO_2)_4(PO_4)_2]_n^{2n-}$ layer, topologically described as a distorted (4,4) net,[12] which is further perforated by eight-membered rings to form pores with an effective cross-section of ca. 2.5 × 2.5 Å (Figure 3).

Table 2. Bond lengths (in Å) for the two-dimensional $[(VO_2)_4(PO_4)_2]_n^{2n-}$ anionic layer; symmetry codes used to generate equivalent atoms: (i) $1-x, y, 1/2-z$, (ii) $-x, y, 1/2-z$, (iii) $x, -1+y, z$, (iv) $1-x, 1+y, 1/2-z$

V(1)−O(9)	1.932(3)	V(3)−O(1)^{ii}	1.855(3)
V(1)−O(10)	1.932(3)	V(3)−O(5)	2.426(3)
V(1)−O(11)	1.841(3)	V(3)−O(5)^{ii}	1.912(3)
V(1)−O(12)	1.877(3)	V(3)−O(6)	1.589(3)
V(1)−O(12)^{i}	2.451(3)	V(3)−O(7)^{iii}	1.918(3)
V(1)−O(15)	1.585(3)	V(3)−O(8)	1.905(3)
V(2)−O(1)	1.857(3)	V(4)^{iv}−O(11)	1.868(3)
V(2)−O(1)^{ii}	2.462(3)	V(4)^{iv}−O(12)^{i}	1.877(3)
V(2)−O(2)	1.933(3)	V(4)^{iv}−O(13)^{iv}	1.908(3)
V(2)−O(3)	1.911(3)	V(4)^{iv}−O(14)	1.923(3)
V(2)−O(4)	1.590(3)	V(4)^{iv}−O(16)^{iv}	1.583(3)
V(2)−O(5)	1.875(3)		

Table 3. Bond angles (in degrees) for the two-dimensional $[(VO_2)_4(PO_4)_2]_n^{2n-}$ anionic layer; symmetry codes used to generate equivalent atoms: (i) $1-x, y, 1/2-z$, (ii) $-x, y, 1/2-z$

O(9)−V(1)−O(10)	90.38(12)	O(1)^{ii}−V(3)−O(5)	79.63(11)
O(9)−V(1)−O(12)^{i}	79.07(11)	O(1)^{ii}−V(3)−O(5)^{ii}	80.07(12)
O(10)−V(1)−O(12)^{i}	77.18(11)	O(1)^{ii}−V(3)−O(7)^{iii}	157.00(12)
O(11)−V(1)−O(9)	89.62(12)	O(1)^{ii}−V(3)−O(8)	89.83(12)
O(11)−V(1)−O(10)	156.61(13)	O(5)^{ii}−V(3)−O(5)	78.66(12)
O(11)−V(1)−O(12)^{i}	79.87(11)	O(5)^{ii}−V(3)−O(7)^{iii}	88.26(12)
O(11)−V(1)−O(12)	80.88(12)	O(6)−V(3)−O(1)^{ii}	102.61(15)
O(12)−V(1)−O(9)	156.87(12)	O(6)−V(3)−O(5)	177.66(14)
O(12)−V(1)−O(10)	90.20(12)	O(6)−V(3)−O(5)^{ii}	100.99(14)
O(12)−V(1)−O(12)^{i}	78.52(12)	O(6)−V(3)−O(7)^{iii}	99.01(15)
O(15)−V(1)−O(9)	100.07(14)	O(6)−V(3)−O(8)	100.50(14)
O(15)−V(1)−O(10)	99.54(14)	O(7)^{iii}−V(3)−O(5)	78.68(11)
O(15)−V(1)−O(11)	103.49(15)	O(8)−V(3)−O(5)	80.09(11)
O(15)−V(1)−O(12)	102.64(14)	O(8)−V(3)−O(5)^{ii}	157.78(12)
O(15)−V(1)−O(12)^{i}	176.56(13)	O(8)−V(3)−O(7)^{iii}	93.88(13)
O(1)−V(2)−O(1)^{ii}	78.52(12)	O(11)−V(4)^{iv}−O(12)^{i}	80.20(12)
O(1)−V(2)−O(2)	157.49(13)	O(11)−V(4)^{iv}−O(13)^{iv}	88.85(12)
O(1)−V(2)−O(3)	89.39(12)	O(11)−V(4)^{iv}−O(14)	157.37(12)
O(1)−V(2)−O(5)	80.98(12)	O(12)^{i}−V(4)^{iv}−O(13)^{iv}	156.73(12)
O(2)−V(2)−O(1)^{ii}	79.47(11)	O(12)^{i}−V(4)^{iv}−O(14)	89.48(12)
O(3)−V(2)−O(1)^{ii}	79.03(11)	O(13)^{iv}−V(4)^{iv}−O(14)	93.12(12)
O(3)−V(2)−O(2)	90.99(12)	O(16)^{iv}−V(4)^{iv}−O(11)	104.01(14)
O(4)−V(2)−O(1)	103.03(14)	O(16)^{iv}−V(4)^{iv}−O(12)^{i}	101.70(14)
O(4)−V(2)−O(1)^{ii}	178.42(13)	O(16)^{iv}−V(4)^{iv}−O(13)^{iv}	100.84(14)
O(4)−V(2)−O(2)	99.01(15)	O(16)^{iv}−V(4)^{iv}−O(14)	97.75(14)
O(4)−V(2)−O(3)	100.63(15)		
O(4)−V(2)−O(5)	102.17(15)		
O(5)−V(2)−O(1)^{ii}	78.31(11)		
O(5)−V(2)−O(2)	90.05(12)		
O(5)−V(2)−O(3)	156.72(13)		

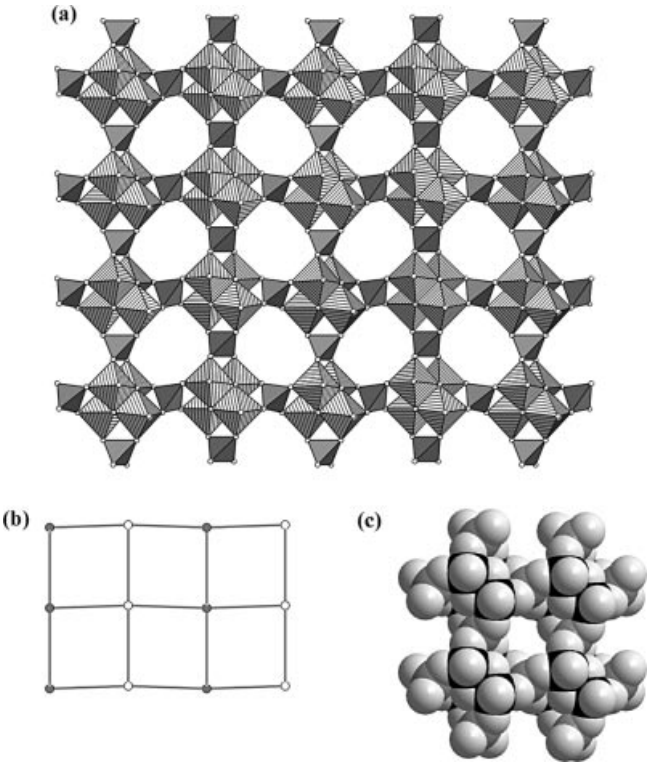

Figure 3. (a) View along the *c* direction of a polyhedral representation of the $[(VO_2)_4(PO_4)_2]_n^{2n-}$ anionic layer, (b) topological representation of the anionic layer which describes a typical (4,4) net (the grey- and white-filled nodes represent the two distinct tetrametallic SBUs), (c) space-fill representation of a portion of the anionic layer showing the pores which have a cross-section of about 2.5 × 2.5 Å

Charge-balancing and space-filling 4,4′-bipyridinium cations are positioned above and below the anionic $[(VO_2)_4(PO_4)_2]_n^{2n-}$ layers, just over the previously mentioned pores (Figure 4). These cations are further connected to the layers through two very strong and highly directional N^+−H···O hydrogen bonds, thus acting as a hydrogen-bonded pillar. The caption of Figure 5 contains further details of the hydrogen-bonding geometry.

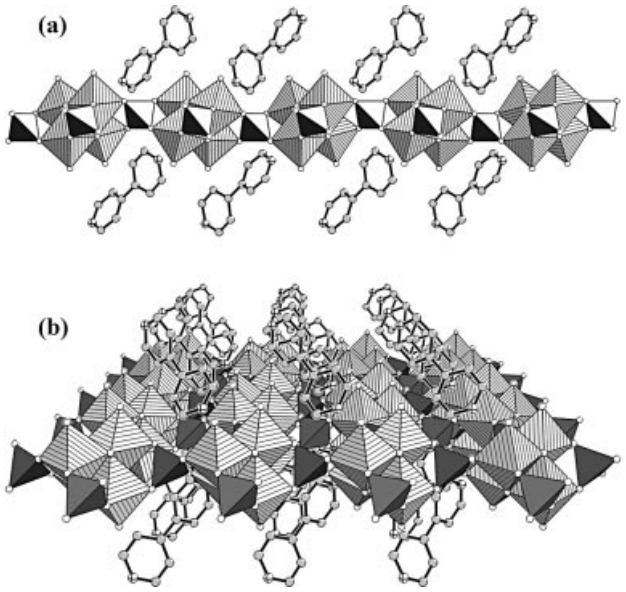

Figure 4. Perspective views along the (a) *b* direction and (b) towards the (100) plane showing the distribution of the 4,4′-bipyridinium cations placed above and below the $[(VO_2)_4(PO_4)_2]_n^{2n-}$ anionic layer

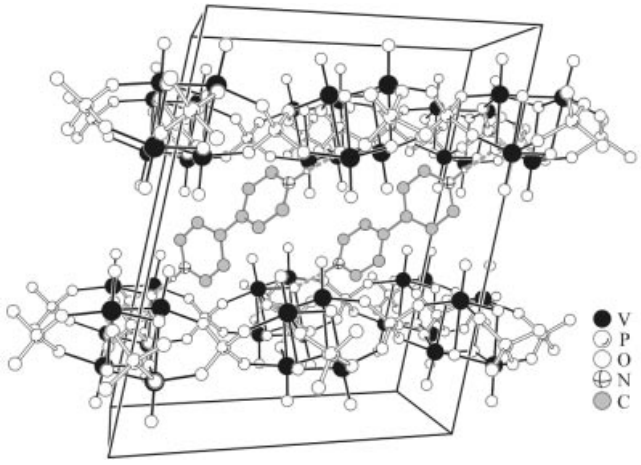

Figure 5. Unit cell contents showing the pillar nature of the interlayer 4,4′-bipyridinium cations through two strong $N^+-H\cdots O$ hydrogen bonds (dashed lines); hydrogen-bonding geometry: N(1)−H(98)···O(12)[i] with *d*(D−H) = 0.976(10) Å, *d*(H···A) = 1.772(12) Å, *d*(D···A) = 2.746(5) Å and <(DHA) = 176(5)°, N(2)−H(99)···O(5)[ii] with *d*(D−H) = 0.974(10) Å, *d*(H···A) = 1.779(12) Å, *d*(D···A) = 2.750(5) Å and <(DHA) = 175(5)°; symmetry codes used to generate equivalent atoms: (i) $1-x$, $1+y$, $1/2-z$. (ii) x, $-y$, $1/2+z$

Solid-State MAS NMR Spectroscopy

The ^1H, ^{13}C, ^{31}P and ^{51}V NMR spectra fully support the crystal structure. Fast (30 kHz) sample spinning averages out the $^1H-^1H$ dipolar interaction, leading to a highly resolved ^1H MAS NMR spectrum (Figure 6a). The 4,4′-bipyridinium cation contains three magnetically nonequivalent ^1H nuclei, labelled H_a, H_b and H_c, which resonate at ca. 15.5, 9.3 (shoulder) and 8.8 ppm, respectively. The $(H_b + H_c)/H_a$ intensity ratio is 4, in accordance to the expected site populations. The ^{13}C CP/MAS NMR spectrum exhibits peaks at ca. 150.6, 145.0 and 124.7 ppm, which are assigned to C_a, C_b and C_c, respectively (Figure 6b). Together, the ^1H and ^{13}C NMR spectra confirm the integrity of the 4,4′-bipyridinium cation.

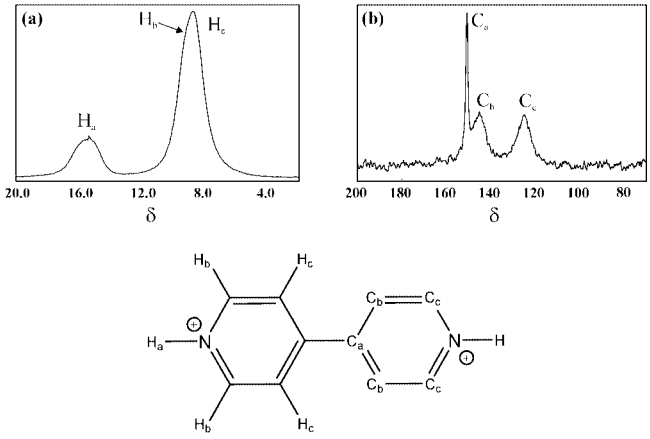

Figure 6. (a) ^1H MAS and (b) ^1H-^{13}C CP MAS NMR spectra, showing the assignment of ^1H and ^{13}C resonances

The ^{31}P MAS NMR spectrum consists of a single peak centred at about −5.2 ppm with a shoulder at about −6.8 ppm which was deconvoluted into three resonances at −6.4, −5.5 and −4.5 in a 1:2:1 intensity ratio, respectively. This is in good agreement with the crystal structure (Figure 7).

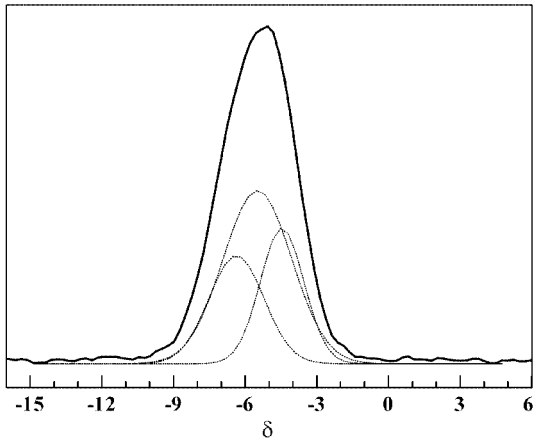

Figure 7. Experimental and simulated ^{31}P MAS NMR spectra

Because of relatively large chemical shift anisotropy, the ^{51}V MAS NMR spectrum exhibits strong spinning sidebands even with MAS at 30 kHz. Three peaks are observed at −580.1, −593.4 and −599.2 ppm in a 2:1:1 intensity ratio, respectively. Since the crystal structure calls for the presence of four nonequivalent V sites, we assume that the peak

at δ = −579.9 ppm consists of two overlapping resonances (Figure 8).

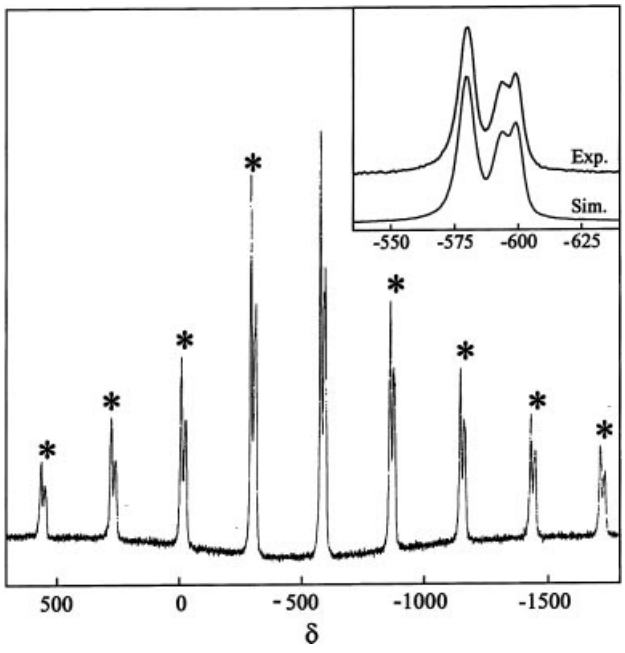

Figure 8. ^{51}V MAS NMR spectrum; the inset shows a magnification of the isotropic peaks (top) and a simulation (bottom) performed with Lorentzian-Gaussian lines (a fair assumption because the second-order quadrupole effects are not significant); asterisks depict spinning sidebands

Thermal Analysis

Thermal treatment reveals that **I** is stable up to ca. 370 °C, as no weight losses were registered. In the 370−800 °C temperature range, the compound undergoes thermal decomposition through five distinct and well-defined steps (as observed in the derivative thermogravimetric analysis), with a total weight loss of 28.3%. This decomposition is attributed to the simultaneous oxidation of the organic component and reduction of half of the V^V centres, leading to the formation of an intermediate inorganic $(V^{IV}_2V^V_2)O_{14}P_2$ phase that contains mixed-valence vanadium centres [72.0% calculated and 71.7% observed residues; Equation (1)]. Between 800 and 900 °C, a continuous weight increase of ca. 1.3% clearly indicates the occurrence of an oxidative process. Indeed, as usually observed in related compounds, traces of oxygen within the apparatus promotes partial oxidation of some V^{IV} centres from the $(V^{IV}_2V^V_2)O_{14}P_2$ intermediate phase, leading to a new mixed-valence phase formulated as $(V^{IV}V^V_3)O_{14.5}P_2$ [73.0% calculated and 73.2% observed residues; Equation (2)].

$$(C_{10}H_{10}N_2)\left[(VO_2)_4(PO_4)_2\right] \xrightarrow[(decomposition\ in\ 5\ steps)]{\Delta} (V^{IV}_2V^V_2)O_{14}P_2 \quad (1)$$

$$(V^{IV}_2V^V_2)O_{14}P_2 \xrightarrow[traces\ of\ O_2]{\Delta} (V^{IV}V^V_3)O_{14.5}P_2 \quad (2)$$

Vibrational Spectroscopy

The IR and Raman spectra contain the most significant diagnostic bands associated with the primary building units of $(C_{10}H_{10}N_2)[(VO_2)_4(PO_4)_2]$. On the one hand, strong bands centred at 990, 970 and 943 cm^{-1} in the IR spectrum (in 976 and 991 in the Raman spectrum) are due to the typical stretching vibrational mode of terminal $V^V{=}O$ double bonds; on the other, bands at 1088 and 1061 cm^{-1} are assigned to the PO_4^{3-} antisymmetric stretching vibrational modes, while those found at 856 and 839 cm^{-1} can be attributed to the related PO_4^{3-} symmetric stretching modes. Several bands observed in the 650−500 cm^{-1} region are also associated with V−O−V stretching vibrational modes, and several intense bands between 1300 and 1640 cm^{-1} arise from the presence of the 4,4′-bipyridinium cations that occupy the interlayer spaces.

Conclusion

A new structure containing 2D anionic $[(VO_2)_4(PO_4)_2]_n^{2n-}$ layers intercalated by 4,4′-bpyH_2^{2+} cations was synthesised by the hydrothermal method and characterised structurally using a variety of techniques. This intercalated phosphovanadate is an important addition to vanadium coordination chemistry as it constitutes the first report of typical $\{V_4O_4\}$ cubane-like clusters. We are currently investigating the intercalation reactions of this compound, particularly the possibility of replacing the 4,4′-bpyH_2^{2+} cations by other organic molecules, and the corresponding structural modifications.

Experimental Section

General: Chemicals were readily available from commercial sources and were used as received without further purification. Syntheses were carried out in PTFE-lined stainless steel reaction vessels (40 cm^3), under autogenous pressure and static conditions in a preheated oven at 140 °C. Reactions took place over a period of 3 days, after which the vessels were removed from the oven and left to cool to ambient temperature before opening. Compounds proved to be air- and light-stable, and insoluble in water and common organic solvents.

Preparation and Structural Characterisation of $(C_{10}H_{10}N_2)[(VO_2)_4(PO_4)_2]$ (I): A yellow suspension containing V_2O_5 (0.140 g, Aldrich), H_3PO_4 (0.450 g, min. 85% Merck) and 4,4′-bipyridine (0.120 g, Fluka) in distilled water (ca. 10 g) was stirred thoroughly for 30 minutes at ambient temperature. The suspension, with a molar composition of ca. 1.0:6.0:1.0:722, respectively, was transferred to the reaction vessel, which was then placed inside the preheated oven. After reacting, the vessel was allowed to cool slowly to ambient temperature to yield a large amount of yellow blocks, which were manually harvested, air-dried for X-ray diffraction analysis and identified as **I**, and a small amount of an unknown pale-green microcrystalline powder. The two phases were readily ultrasonically separated (for 10 minutes), followed by vacuum filtration and washing with copious amounts of distilled water. $C_{10}H_{10}N_2O_{16}P_2V_4$ (based on single-crystal data, 679.90): calcd. C 17.67, N 4.14,

H 1.48; found C 18.07, N 4.26, H 1.49. TGA data (weight losses and increases) and derivative thermogravimetric peaks (DTG; in parenthesis): 370−450 °C, −8.4% (425 °C); 450−800 °C, −19.9% (540, 621, 661 and 771 °C); 800−900 °C, +1.3% (849 °C).

Selected IR and Raman data in cm^{-1}): 1639 vs (1645), 1620 vs (1623), 1488 s, 1459 m, 1417 m, 1375 s (1367), 1340 m, 1088 vs (1074), 1061 vs, 990 vs, 970 vs, 943 s, 856 m, 839 m, 793 s, 654 m, 622 s, 610 m, 590 m, 503 vs.

Characterisation: Elemental analyses for C, H and N were performed on an Exeter Analytical CE-440 Elemental Analyser (University of Cambridge). Samples were combusted under oxygen at 975 °C, with He as the purge gas.
FT-IR spectra were measured from KBr disks (Aldrich, 99%+, FT-IR grade) on a Matson 700 FTIR spectrometer, and FT-Raman spectra were collected on a Bruker RFS 100 with a Nd:YAG coherent laser (λ = 1064 nm).
Thermogravimetric analyses (TGA) were carried out on Shimadzu TGA-50, with a heating rate of 10 °C/min, under nitrogen with a flow rate of 20 cm^3/min.
Powder X-ray diffraction patterns were recorded at room temperature on a Philips X'Pert diffractometer, operating with a monochromated Cu-K_α radiation source at 40 kV and 50 mA. Simulated powder patterns were based on single-crystal data, and calculated with the STOE Win XPOW software package.[13]
^{1}H, ^{13}C, ^{31}P and ^{51}V solid-state NMR spectra were recorded at 400.12, 100.61, 160.0 and 105.24 MHz, respectively, on a Bruker Avance 400 spectrometer. ^{1}H and ^{31}P MAS NMR spectra were recorded with a 30 kHz spinning rate, 40° rf pulses and recycle delays of 6 and 70 s, respectively. ^{1}H- ^{13}C cross-polarisation (CP) MAS NMR spectra were acquired with 4 μs ^{1}H 90° pulses, a contact time of 2 ms and a recycle delay of 5 s. ^{51}V MAS NMR spectra were recorded with short, 0.6 μs (equivalent to 10°), pulses and a recycle delay of 5 s. Chemical shifts are quoted in ppm from TMS (^{1}H and ^{13}C), 85% H_3PO_4 (^{31}P) and $VOCl_3$ (^{51}V).

X-ray Crystallographic Studies: Suitable single crystals were mounted on a glass fibre using perfluoropolyether oil.[14] Data were collected at 180(2) K on a Nonius Kappa charge-coupled device (CCD) area-detector diffractometer (Mo-K_α graphite-monochromated radiation, λ = 0.7107 Å) equipped with an Oxford Cryosystems cryostream and controlled by the Collect software package.[15] Images were processed with the software packages Denzo and Scalepack,[16] and the data were corrected for absorption by the empirical method employed in Sortav.[17] The structure was solved by the direct methods of SHELXS-97[18] and refined by full-matrix least-squares on F^2 using SHELXL-97.[19]

All non-hydrogen atoms were directly located from difference Fourier maps and refined with anisotropic displacement parameters. The crystallographically unique H-atoms associated with the 4-pyridinium groups were also located from difference Fourier maps, and refined with independent isotropic displacement parameters and a common N−H distance restrained to 0.98(1) Å. Hydrogen atoms attached to carbon were located at their idealised positions using the HFIX 43 instruction in SHELXL, and included in the refinement in riding-motion approximation with an isotropic thermal displacement parameter fixed at 1.2 times U_{eq} of the atom to which they are attached. The last difference Fourier map synthesis shows the highest peak (0.641 e·Å^{-3}) located at 1.42 Å from O(11), and the deepest hole (−0.666 e·Å^{-3}) at 0.79 Å from V(2). Cavity dimensions were calculated by overlapping rigid spheres with van der Waals radii for each element: O 1.52 Å, P 1.8 Å and V 2.0 Å. CCDC-221172 contains the supplementary crystallographic data for this paper. These data can be obtained free of charge at www.ccdc.cam.ac.uk/conts/retrieving.html [or from the Cambridge Crystallographic Data Centre, 12 Union Road, Cambridge CB2 1EZ, UK; Fax: (internat.) + 44-1223-336-033; E-mail: deposit@ccdc.cam.ac.uk].

Acknowledgments

We are grateful to FEDER, POCTI (Portugal) and to the Portuguese Foundation for Science and Technology (FCT) for their general financial support, and also for the Ph.D. and postdoctoral research grants Nos. SFRH/BD/3024/2000 (to F. A. A. P.) and SFRH/BPD/9309/2002 (to F.-N. S.).

[1] P. J. Hagrman, R. C. Finn, J. Zubieta, *Solid State Sci.* **2001**, *3*, 745−774.
[2] A. K. Cheetham, G. Ferey, T. Loiseau, *Angew. Chem. Int. Ed.* **1999**, *38*, 3269−3292; G. Centi, F. Trifiro, J. R. Ebner, V. M. Franchetti, *Chem. Rev.* **1988**, *88*, 55−80; F. Garbassi, J. C. J. Bart, F. Montino, G. Petrini, *Applied Catalysis* **1985**, *16*, 271−287.
[3] C. Qin, L. Xu, Y. G. Wei, X. L. Wang, F. Y. Li, *Inorg. Chem.* **2003**, *42*, 3107−3110; Z. Shi, S. H. Feng, L. R. Zhang, G. Y. Yang, J. Hua, *Chem. Mat.* **2000**, *12*, 2930−2935; R. Finn, J. Zubieta, *Chem. Commun.* **2000**, 1321−1322.
[4] Y. J. Lu, R. C. Haushalter, J. Zubieta, *Inorg. Chim. Acta* **1998**, *268*, 257−261; V. Soghomonian, R. C. Haushalter, J. Zubieta, C. J. Oconnor, *Inorg. Chem.* **1996**, *35*, 2826−2830; V. Soghomonian, Q. Chen, R. C. Haushalter, J. Zubieta, *Angew. Chem. Int. Ed., Engl.* **1993**, *32*, 610−612.
[5] F. A. Almeida Paz, Y. Z. Khimyak, A. D. Bond, J. Rocha, J. Klinowski, *Eur. J. Inorg. Chem.* **2002**, 2823−2828; F. A. Almeida Paz, J. Klinowski, *J. Phys. Org. Chem.* **2003**, *16*, 772−782; F. A. Almeida Paz, J. Klinowski, *Chem. Commun.* **2003**, 1484−1485; F. A. Almeida Paz, J. Klinowski, *Inorg. Chem.* **2004**, in press, DOI: 10.1021/ic049523o; F. A. Almeida Paz, J. Klinowski, *Inorg. Chem.* **2004**, in press, DOI: 10.1021/ic049794z; F. A. Almeida Paz, J. Klinowski, *J. Solid. State Chem.* **2004**, in press.
[6] F. A. Almeida Paz, F.-N. Shi, J. Klinowski, J. Rocha, T. Trindade, *Eur. J. Inorg. Chem.* **2004**, DOI: 10.1002/ejic.200400005.
[7] F.-N. Shi, F. A. Almeida Paz, J. Klinowski, J. Rocha, T. Trindade, *Inorg. Chim. Acta* **2004**, submitted.
[8] M. J. Manos, A. L. Tasiopoulos, E. L. Tolis, N. Lalioti, J. D. Woollins, A. M. Z. Slawin, M. P. Sigalas, T. A. Kabanos, *Chem. Eur. J.* **2003**, *9*, 695−703; M. Worle, F. Krumeich, F. Bieri, H. J. Muhr, R. Nesper, *Z. Anorg. Allg. Chem.* **2002**, *628*, 2778−2784; F. L. Jiang, O. P. Anderson, S. M. Miller, J. Chen, M. Mahroof-Tahir, D. C. Crans, *Inorg. Chem.* **1998**, *37*, 5439−5451; W. Plass, *Eur. J. Inorg. Chem.* **1998**, 799−805; W. Plass, *Inorg. Chem.* **1997**, *36*, 2200−2205; D. C. Crans, F. L. Jiang, J. Chen, O. P. Anderson, M. M. Miller, *Inorg. Chem.* **1997**, *36*, 1038−1047; N. P. Luneva, S. A. Mironova, A. E. Shilov, M. Y. Antipin, Y. T. Struchkov, *Angew. Chem. Int. Ed., Engl.* **1993**, *32*, 1178−1179; M. Mikuriya, T. Kotera, F. Adachi, S. Bandow, *Chem. Lett.* **1993**, 945−948; I. Cavaco, J. C. Pessoa, M. T. Duarte, P. M. Matias, R. T. Henriques, *Polyhedron* **1993**, *12*, 1231−1237; D. C. Crans, R. W. Marshman, M. S. Gottlieb, O. P. Anderson, M. M. Miller, *Inorg. Chem.* **1992**, *31*, 4939−4949; F. Bottomley, D. F. Drummond, D. E. Paez, P. S. White, *J. Chem. Soc., Chem. Commun.* **1986**, 1752−1753; F. Bottomley, D. E. Paez, P. S. White, *J. Am. Chem. Soc.* **1985**, *107*, 7226−7227; F. Bottomley, D. E. Paez, P. S. White, *J. Am. Chem. Soc.* **1982**, *104*, 5651−5657; F. Bottomley, P. S. White, *J. Chem. Soc., Chem. Commun.* **1981**, 28−29; Y. Chang, Q.

Chen, M. I. Khan, J. Salta, J. Zubieta, *J. Chem. Soc., Chem. Commun.* **1993**, 1872−1874; H. Rieskamp, P. Gietz, R. Mattes, *Chem. Ber.* **1976**, *109*, 2090.
[9] F. H. Allen, *Acta Crystallogr., Sect. B* **2002**, *58*, 380−388.
[10] H. P. Zhu, Q. T. Liu, C. N. Chen, D. X. Wu, *Inorg. Chim. Acta* **2000**, *306*, 131−136; S. A. Duraj, M. T. Andras, B. Rihter, *Polyhedron* **1989**, *8*, 2763−2767; A. A. Pasynskii, I. L. Eremenko, A. S. Katugin, G. S. Gasanov, E. A. Turchanova, O. G. Ellert, Y. T. Struchkov, V. E. Shklover, N. T. Berberova, A. G. Sogomonova, O. Y. Okhlobystin, *J. Organomet. Chem.* **1988**, *344*, 195−213; J. Darkwa, J. R. Lockemeyer, P. D. W. Boyd, T. B. Rauchfuss, A. L. Rheingold, *J. Am. Chem. Soc.* **1988**, *110*, 141−149.
[11] S. Boudin, A. Guesdon, A. Leclaire, M. M. Borel, *Int. J. Inorg. Mater.* **2000**, *2*, 561−579.
[12] A. F. Wells, *Structural Inorganic Chemistry Fourth ed.,* Clarendon Oxford University Press, **1975**.
[13] STOE, *Win XPOW THEO Version 1.15*, STOE & Cie GmbH, **1999**.
[14] T. Kottke, D. Stalke, *J. Appl. Crystallogr.* **1993**, *26*, 615−619.
[15] R. Hooft, *Collect: Data Collection Software, Nonius B. V.,* Delft, The Netherlands, **1998**.
[16] Z. Otwinowski, W. Minor, *Methods in Enzymology*, Vol. 276, *Macromolecular Crystallography, Part A* (Eds.: C. W. Carter Jr., R. M. Sweet), Academic Press, New York, **1997**, pp. 307.
[17] R. H. Blessing, *J. Appl. Crystallogr.* **1997**, *30*, 421; R. H. Blessing, *Acta Crystallogr., Sect. A* **1995**, *51*, 33−38.
[18] G. M. Sheldrick, *SHELXS-97*, *Program for Crystal Structure Solution*, University of Göttingen, University of Göttingen, **1997**.
[19] G. M. Sheldrick, *SHELXL-97*, *Program for Crystal Structure Refinement*, University of Göttingen, University of Göttingen, **1997**.

Received March 29, 2004
Early View Article
Published Online June 17, 2004

